Dalton Transactions

ROYAL SOCIETY OF CHEMISTRY

PAPER

View Article Online
View Journal | View Issue

Check for updates

Cite this: *Dalton Trans.*, 2023, **52**, 4494

Penta-coordinated or -valent: the nature of the chemical bond of some Ti–C–Al compounds†

J. Saßmannshausen

Received 18th January 2023,
Accepted 7th March 2023

DOI: 10.1039/d3dt00164d

rsc.li/dalton

Detailed DFT calculations of the published [CpTi(μ^2-Me)(μ^2-NPPh$_3$)(μ^5-C)(μ^2-AlMe$_2$)$_2$(AlMe$_2$)(AlMe$_3$)] **1** revealed the triple-bond nature of the Ti–C bond and thus being a methide carbon with 5 surrounding ligands. This finding was further corroborated by the derivates [CpTi(μ^2-Me)(μ^2-NPPh$_3$)(μ^4-C)(μ^2-AlMe$_2$)$_2$(AlMe$_2$)] **3**, which has one AlMe$_3$ ligand "removed" compared to **1**, and [CpTi(μ^2-NPPh$_3$)(SiMe$_3$)(μ^3-C)(μ^2-AlMe$_2$)(AlMe$_2$)] **4**, where the –AlMe$_2$ moiety has been replaced by a non-coordinating SiMe$_3$ one. Detailed electronic investigations (QTAIM, NBO, ETS-NOVC) suggest a Ti–C triple bond, with one AlMe$_2$ moiety covalently bound to the carbon and the remaining three AlMe$_x$ moieties interacting more in a Lewis acid–base fashion. Consequently, this is a penta-coordinated carbon and not, as the geometry would suggest, a penta-valent one.

Introduction

A detailed understanding of the nature of a bond between the elements in a compound is of fundamental importance for the properties of the molecule, in particular for a catalyst.

Take for example carbon, which as the first element of group 4, has normally a coordination number of four originating from the four sp^3 orbitals creating four available orbitals for bonding. The simplest example for this kind of bonding would be CH_4 where the 1s orbital of the hydrogens are interacting with one of the sp^3 orbitals of the carbon forming a σ-bond, creating the familiar tetrahedral shape of the molecule. Lower hybridizations modes are possible utilizing only two or one p-orbitals to result in sp^2 and sp orbitals, respectively, where the remaining p-orbitals are usually engaged in π type bonds. This concept is incomplete as carbon can expand its coordination sphere above 4 to for example 5, as reported for the cationic compound Li_5C^+ as early as 1976 (see in text of ref. 1). This structure was later subject to DFT investigations by Schleyer 1982.[1,2] Here the sp^2 hybridized orbitals are bonding three of the Li ligands whereas the remaining p-orbital is binding the remaining two Li ligands in a σ-allyl type nearly linear 3 centre 2 electron (3c2e) bond.[3] This way, the resulting overall wavefunction for this particular orbital combination is lowered, compared with the individual orbitals. These kinds of compounds can be considered as penta-valent, as the atom–atom interaction is that of a valence bond, with the carbon to be considered hypercoordinated since it has eight valence electrons to bond to the five lithium atoms. Unfortunately, Schleyer *et al.* did not report the electronic structure of the Li_5C^+ compound at the time.

More recently Merino *et al.* published an excellent comprehensive review of planar tetra- and penta-coordinated carbon compounds, including some quite stunning movies of the molecular dynamics of some of the investigated compounds.[4,5]

Addressing these observations and unearthing the underlying electronic structure is not only a pure academic question but one of fundamental importance.[5] In general, understanding the intrinsic steps of a reaction, which often is governed by electronic effects and hypervalent/hypercoordinated elements,[6–9] is of great importance as it helps to tailor-make catalysts which in turn might be more efficient as well.

To this end, we have been interested in these kind of investigations for some years now and have often discovered unexpected electronic properties.[10–16] Hence, the report from Stephan in 2000 about the unusual five-fold coordinate sphere of the Ti–Al–C compound **1** was an interesting subject to explore.[17–19] Here, we report the electronic nature of the carbon atom which is surrounded by five ligands, clearly in breach of the more common 4 'bonding' carbon.

Results and discussion

Validation of the employed level was done by optimising the geometry of the solid state structure, and relevant parameters are in good agreement between the observed and calculated structure (Table S1†). Minor details in bond length and angles are most likely due to the difference between the observed solid state structure and the calculated gas-phase one. During

Imperial College London, UK. E-mail: j.sassmannshausen@imperial.ac.uk

† Electronic supplementary information (ESI) available. See DOI: https://doi.org/10.1039/d3dt00164d

Table 1 Relevant metrics between **1**, **1-dft**, and **2**. Distances in Å, angles in degree

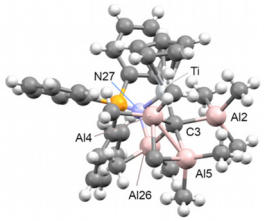

1

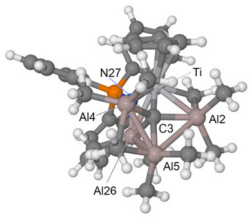

1-dft

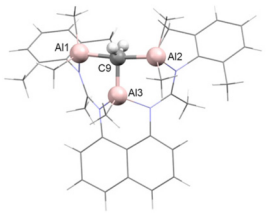

2

	1	**1-dft**	**2**	
d(C3–Al2)	2.095(3)	2.08	*d*(Al1–C9)	2.098(2)
d(C3–Al4)	2.087(3)	2.12	*d*(Al2–C9)	2.100(2)
d(C3–Al5)	2.121(3)	2.11	*d*(Al3–C9)	1.958(2)
d(C3–Al26)	2.150(3)	2.12		
∢(Ti–C3–Al4)	104.81	106.45	∢(Al1–C9–Al2)	173.10(11)
∢(Ti–C3–Al5)	175.80	175.11	∢(Al1–C9–Al3)	94.47(8)
∢(Al2–C3–Al4)	130.72	129.31	∢(Al2–C9–Al3)	92.41
∢(Al2–C3–Al26	114.77	114.94		
∢(Al4–C3–Al26)	114.37	115.16		
∑(Al2–Al4–Al26–C3)	359.86	359.41		

the preparation of this manuscript Villegas-Escobar *et al.* reported a similar trigonal–bipyramidal carbon with three aluminium and two hydrogens atoms around the carbon (*cf.* Table 1).[20]

Their metrics are very close to the one from Stephan's compound and are listed in Table 1 for comparison.

In both cases, the geometry is close to a perfect trigonal–bipyramidal structure with the Ti(Al)–C–Al angle being 175.11° (**1-dft**), 175.80° (**1**) and 173.10(11)° (**2**), respectively. The C–Al bond distances are around 2.11 Å. The in-plane distances between the carbon and aluminium are slightly shorter than the carbon-apical ones. Some distortion of the ideal 120° can be observed reflecting the different ligands in the plane (aluminium in **1** and **1-dft**, and aluminium and hydrogen in **2**). Bearing in mind the differences between both compounds, the overall geometry is remarkable similar.

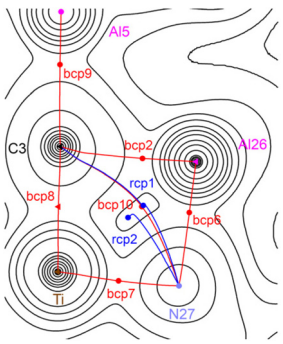

Fig. 1 Electron density plot through Ti, C3 and Al26 with N27 and Al5 being out of plane.

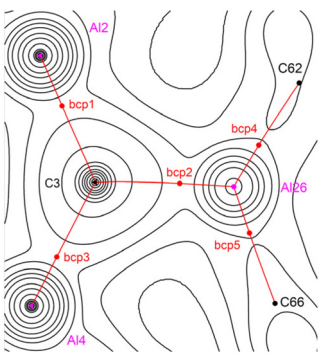

Fig. 2 Electron density plot through Al2, C3 and Al4 with Al26, C62 and C66 being out of plane.

Electronic structure analysis

In order to obtain a more detailed understanding of the nature of the interactions between carbon and aluminium in **1-dft**, QTAIM and NBO analysis were performed.[3] We obtained bond paths between carbon and all of the five surrounding ligands for **1-dft** as illustrated in Fig. 1 and 2, and relevant parameters summarized in Table 2. Plots for the Laplacians of the electron-density are provided in the ESI.†

Judging from the values of the bond critical points bcp1–3 and bcp9, the central carbon is bound equally to the aluminium atoms. This is further corroborated by the Laplacian of these points which are very similar and suggesting the expected an open-shell, ionic interaction.[21] However, the values of the Ti–C bcp8 are nearly twice as strong as the C–Al ones. Thus, more electron density can be expected between these two atoms compared with the C–Al interaction. The slightly lower value of the Laplacian of bcp9 would also suggest a less ionic interaction. This raises some doubts about

Table 2 Electron densities and Laplacians of **1-dft**

	$\rho(r)$	$\nabla^2\rho(r)$
bcp1	0.0588	−0.0551
bcp2	0.0555	−0.0502
bcp3	0.0552	−0.0517
bcp6	0.0567	−0.0871
bcp7	0.1226	−0.0993
bcp8	0.1286	−0.0452
bcp9	0.0556	−0.0534
bcp10	0.0377	−0.0103

Table 3 Summary of bond properties of **1-dft**

	BCP (total density)		NBCP (NAO atomic densities)		Natural binding index[a]	Wiberg
	$\rho(r)$	$\nabla^2\rho(r)$	$\rho(r)$	$\nabla^2\rho(r)$		
Ti–C3	0.1286	0.1809	0.1358	0.1965	1.2194	1.4868
C3–Al2	0.0588	0.2206	0.0570	0.2123	0.5542	0.3071
C3–Al4	0.0552	0.2068	0.0579	0.2053	0.5574	0.3107
C3–Al5	0.0556	0.2137	0.0616	0.2209	0.6119	0.3744
C3–Al26	0.0555	0.2010	0.0523	0.1835	0.4994	0.2494

[a] NCU strength parameters

Table 4 Summary of atomic properties of **1-dft**

	Bader charge	Natural charge	Wiberg index	NLMO/NPA bond orders
Ti		0.87250	4.5537	5.2905
C3	−2.63525	−1.88537	3.0970	1.8741
Al2	2.31071	1.80942	1.9592	1.9195
Al4	2.32283	1.77598	2.0165	1.9736
Al5	2.32471	1.65577	2.1941	2.0046
Al26	2.34443	1.96122	1.7349	1.7707

the potential electronic similarities between **1-dft** and **2**. Indeed, detailed NBO analysis reveals the following picture:

- The carbon is sp hybridized
- The Ti–C bond is a triple bond
- The remaining sp hybrid orbital is bonding Al5

The remaining three aluminium atoms are interacting in such a way that a suitable Ti–C π-bond is donating electron density into an empty p-orbital of the aluminium atom (*cf.* Fig. 3).

Further plots of all relevant Ti–C–Al orbital interactions are in the ESI.† A summary of the various metrics further corroborating the multibonding nature of the Ti–C bond is given in Table 3, and Bader and NBO charges of selected atoms in Table 4.

In all cases, we note that the values for the Ti–C bond are significantly higher than for the C–Al bonds, further corroborating the multiple bond character of the Ti–C bond.

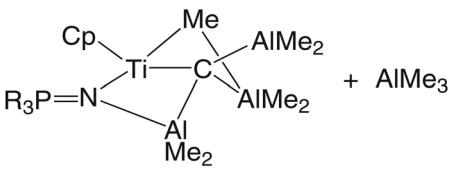

5

R = ^{i}Pr

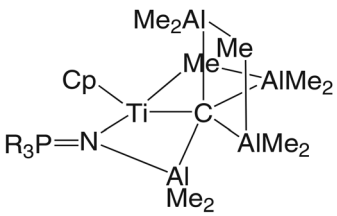

6

instead of the μ^2-NPPh$_3$ moiety, which is in equilibrium with AlMe$_3$ (eqn (1)).[17]

Derivatives

To gain more insight into the nature of the Ti–C bond and to further corroborate our hypothesis, we were looking into the similar compounds, which can be seen as derivates of **1**. In particular, a derivative of **1** which has a bridging μ^2-NP^{i}Pr$_3$

Thus, we were investigating [CpTi(μ^2-Me)(μ^2-NPPh$_3$)(μ^4-C)(μ^2-AlMe$_2$)$_2$(AlMe$_2$)] **3**, which is similar to **5** and [CpTi(μ^2-NPPh$_3$)(SiMe$_3$)(μ^3-C)(μ^2-AlMe$_2$)(AlMe$_2$)] **4**, in which the N-AlMe$_2$ moiety has been replaced with a non-coordinating –SiMe$_3$ one. This way, we are 'stripping' the Ti–C bond from all the non-co-

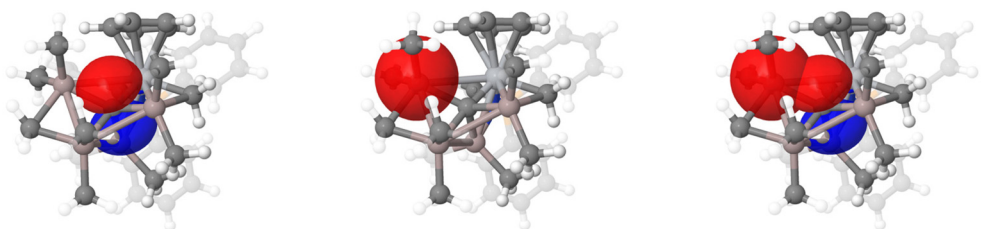

Fig. 3 Typical interaction between the Ti–C π-bond and an empty Al orbital of predominantly s-shape.

valently bounded Al ligands to investigate the true nature of that bond. Additionally, next to the already employed QTAIM and NBO methods, we are also utilizing ETS-NOVC[22–25] to get a different view of this bond. This way, we hopefully remove any kind of bias which might be inherited to the used methods. For better comparison, some relevant metrics of **1-dft**, **3** and **4** are summarised in Table 5.

Inspection of Table 5 indicates the release of pressure of the C3–Al4–C14–Al5 butterfly shaped ring, going from **1-dft** to **3** and finally **4**, as evident from the dihedral angle of the ring going from −17.49° to finally −10.51°. The position of the ring is also shifting, as evident from the shortening of the Ti–C3–Al5 angle from 175.11° Å to 134.58°. These changes are concomitant with a shortening of the Ti–C3 bond from 1.947 Å to 1.757 Å. For comparison, we also calculated Al_2Me_3 at the same level of theory. Here we found an average Al–μCH_3 bond distance of 2.14 Å with an Al–Al distance of 3.394 and a dihedral angle of −11.27°. So far, our hypothesis of a Ti–C triple bond with one covalently[26] bound terminal $AlMe_2$ and the remaining three Al moieties surrounding this bond and are interacting in a dative[27] bond fashion with Ti–C3 triple bond.

As before, we conducted QTAIM and NBO analysis and the relevant data are collated in Tables 6 and 7, respectively.

As evident from Table 6, the electron density $\rho(r)$ of the Ti–C3 bond critical point is increasing, concomitant with a decrease of the Laplacian $\nabla^2\rho(r)$ of that point. This would further corroborate our hypothesis that the three Al atoms in the plane of trigonal–bipyramidal (Al4, Al5 and Al26) are coordinated *via* a dative bond to the Ti–C triple bond, rather than *via* a covalent bond to the carbon. This is also confirmed by looking at the NBO donor–acceptor interactions, which indicate that a Ti–C π bond is donating electron density into an empty orbital of these aluminium ligands. Drawings of these interactions can be found in the ESI.†

To finish off our detailed investigations, we were also looking into ETC-NOVC to see if our hypothesis is correct, or the wrong conclusions are drawn due to a biased method. This analysis was conducted by first computing the whole molecule (closed shell) and then the two fragments where the Ti–C bond has been broken. In light that the original compound **1** is diamagnetic, which does imply a Ti^{4+} species, we arrived to the same conclusion as Stephan[17] and assumed a Ti–C triple bond. Thus, both fragments were treated as open shell with a multiplicity of 4. Furthermore, we made sure the C3–Al4–Al5–C14 ring remains intact, assuming a structure similar to Al_2Me_3. This leads to three dominant interactions: one which could be assigned to be of σ and two broadly to be of π character. We noticed that these orbitals are not localised but seem to be highly delocalised, in particular in the direction of the in-plane Al atoms. This is more dominant in **1-dft** compared to **4** (*cf.* Fig. 4).

Fig. 4 shows the NOVC pairs which are making up the shown bonds. For example, for **4** the NOVC pair 1–514 is made up of the pair 1 with orbitals 1 and 1025; and pair 514 with orbitals 1026 and 2050 (*cf.* ESI page 40†). The overall interaction

Table 6 QTAIM results of **1-dft**, **3** and **4**

	BCP (total density) **1-dft**		BCP (total density) **3**		BCP (total density) **4**	
	$\rho(r)$	$\nabla^2\rho(r)$	$\rho(r)$	$\nabla^2\rho(r)$	$\rho(r)$	$\nabla^2\rho(r)$
Ti–C3	0.1286	0.1809	0.1755	−0.0483	0.1951	−0.0522
C3–Al4	0.0552	0.2068	0.0552	−0.0537	0.0672	−0.0709
C3–Al5	0.0556	0.2137	0.0656	−0.0687	0.0447	−0.0393
C3–Al26	0.0555	0.2010	0.0577	−0.0539	n.a.	n.a.

Table 5 Metrics summary of **1-dft**, **3** and **4**. Distances in Å, angles in degree

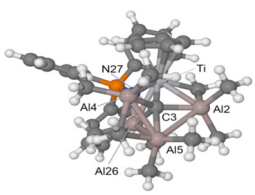

1-dft

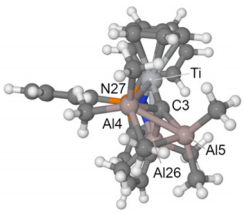

3

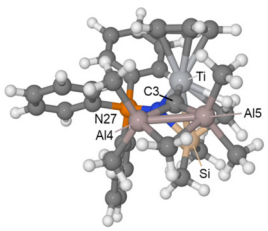

4

	1-dft	**3**	**4**
d(Ti–C3)	1.947	1.807	1.757
d(Ti–Al26)	2.743	2.692	n.a.
d(Ti–N27)	1.919	1.937	2.119
d(Al4–Al5)	2.636	2.667	2.631
d(C3–Al4)	2.119	2.079	1.996
d(C3–Al5)	2.108	2.021	2.010
d(C3–Al26)	2.119	2.097	n.a.
∢(Ti–C3–Al26)	84.72	86.84	n.a.
∢(Ti–C3–Al5)	175.11	161.25	134.58
∢(Ti–C3–Al4)	106.45	107.66	141.46
∢(Al4–C3–Al5)	129.31	81.15	82.08
∢(Al4–C3–Al26)	115.16	121.13	n.a.
∢(Al5–C3–Al4–C14)	−17.49	−21.71	−10.51

Table 7 Selected charges for QTAIM and NBO analysis of **1-dft**, **3** and **4**

	Bader charge **1-dft**	Bader charge **3**	Bader charge **4**	Natural charge **1-dft**	Natural charge **3**	Natural charge **4**
Ti				0.8725	1.1971	0.8288
C3	−2.6353	−2.2732	−1.9345	−1.8854	−1.5384	−1.2619
Al4	2.3228	2.3306	2.3444	1.7760	1.6515	1.6365
Al5	2.3247	2.3354	2.3380	1.6558	1.6462	1.6305
Al26	2.3444	2.3529	n.a.	1.9612	1.7792	

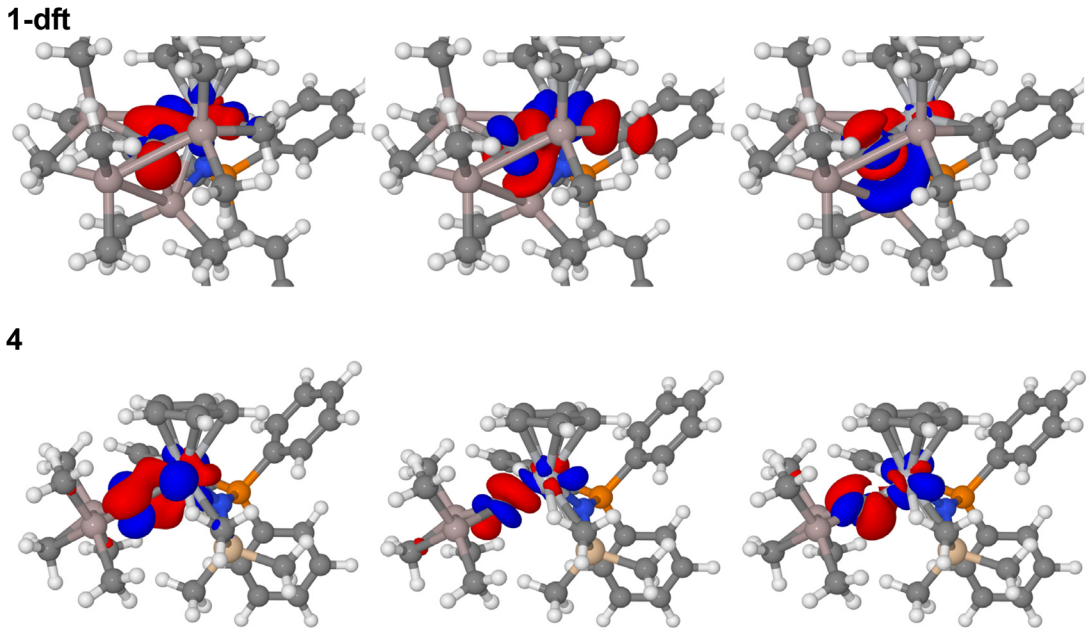

Fig. 4 NOVC pairs of **1-dft** (top) and **4** (bottom). The individual pairs of orbitals making up these interactions are shown in the ESI† for more information.

is shown in Fig. 4 and resembles that of a π bond. In general for **4** it is very easy to identify the various Ti–C σ and the two π bonds, whereas for **1-dft** this is more complex due to the delocalisation of the bonds. However, this is in line with our hypothesis about the Ti–C triple bond, which is donating electron density into suitable Al orbitals for Al2, Al4, and Al5. As a consequence of this electron donation, the electron density between Ti and C3 will be decreased going from **4** to **1-dft** *via* **3**, which also explains the apparent paradox of C3 having a higher charge in **1-dft** compared to **4**: as clearly visible in Fig. 4, the bonding orbitals are more located on C3 than Ti (*cf.* NOVC pair 2–565), thus C3 having a higher electron density, compared with NOVC pair 2–516, where the electron density is more between C3 and Ti as expected for a more traditional triple bond.

Conclusion

From the presented data we can draw the following conclusion: although the geometrical arrangement is that of a trigonal–bipyramidal one, detailed electronic analysis shows clearly a Ti–C3 triple-bond, *i.e.* a methide carbon. Analysis of the C3–Al5 bond, *i.e.* at the other 'tip' of the trigonal–bipyramidal geometry, is more of single bond character in line with the originally proposed methide carbon. The remaining three aluminium atoms are in the plane of the geometry and show a dative bond between a suitable Ti–C bond and an empty Al orbital of suitable shape. The different values for Al26, compared with Al2 and Al4, can be explained by the additional interaction with N27 (*cf.* Fig. 1) and thus some of the electron density demand is satisfied *via* that interaction. This conclusion is further corroborated from the derivatives **3** and **4**, which clearly show an expected trend. In conclusion, support for the original description of the C3 atom in **1** as a *penta-coordinated* rather than *penta-valent* carbon, as found in **2**, has been obtained.[17] Detailed electronic analysis needs to be done for these unusual, curious trigonal–bipyramidal shaped carbons to obtain the true electronic nature of these carbons.

Computational details

All calculations were performed at using the PBE0 functional[28,29] in combination of a mixed basis set consisting

of Pople's 6-311G(d,p) basis set[30] for all elements apart from Ti, where the Stuttgart–Dresden effective core potential was used.[31] This mixed basis set is abbreviated ecp11 and an expansion of the previously employed ecp1 mixed basis set.[32] The PBE0 functional was found to give good results for transition metal complexes, specially in combination with Grimme's DFT-D method.[33,34]

All calculations were performed using GAMESS-US versions 2019-R1 and 2021-R2 using a standard grid setting.[35,36] The optimised structure was subject to a numerical Hessian calculation to verify the nature of the structure being a true minimum (no imaginary frequencies).

For the ETS-NOVC properties calculation, we were using the DZVP all electron basis[37] set instead of the effective core potential one. The larger Sapporo-DKH3-DZP basis set in combination with the all-electron scalar relativity treatment employing the local unitary transformation modification (keyword RELWFN = LUT-IOTC) with a large grid (keywords nrad = 125 nleb = 1202) as implemented in GAMESS-US were used for the Quantum Theory of Atoms in Molecules (QTAIM),[38] and Natural Bond Orbital (NBO).[39,40] This way, we hope to obtain a comprehensive understanding of the way the atoms in this molecule are interacting with each other. For visualisation of the QTAIM analysis AIM2000[41,42] was utilized, the various orbitals were generated using Jmol.[43] For the ETS-NOVC analysis the program Multiwfn, version 3.8, was employed.[44] All of the raw data of the computed compounds **1-dft**, **3**, and **4** are available free to download from **https://doi.org/10.5281/zenodo.7683030**.

Conflicts of interest

There are no conflicts to declare.

Acknowledgements

J. S. is greatly in debt to Jennifer Green for her initial help with DFT calculations, her inspiration and continuous support, and also for the late Malcolm Green for his encouragement to go outside the well trotted paths.

References

1 E. D. Jemmis, J. Chandrasekhar, E. U. Wuerthwein, P. v. R. Schleyer, J. W. Chinn, F. J. Landro, R. J. Lagow, B. Luke and J. A. Pople, *J. Am. Chem. Soc.*, 1982, **104**, 4275.
2 P. v. R. Schleyer, E. U. Wuerthwein, E. Kaufmann, T. Clark and J. A. Pople, *J. Am. Chem. Soc.*, 1983, **105**, 5930.
3 I. Fernández, E. Uggerud and G. Frenking, *Chem. – Eur. J.*, 2007, **13**, 8620.
4 Z.-h. Cui, V. Vassilev-Galindo, J. L. Cabellos, E. Osorio, M. Orozco, S. Pan, Y.-h. Ding and G. Merino, *Chem. Commun.*, 2017, **53**, 138.
5 V. Vassilev-Galindo, S. Pan, K. J. Donald and G. Merino, *Nat. Rev. Chem.*, 2018, **2**, 0114.
6 W. Buchowicz, B. Herbaczynka, L. B. Jerzykiewicz, T. Lis, S. Pasynkiewicz and A. Pietrzykowski, *Inorg. Chem.*, 2012, **51**, 8292.
7 W. Ahlers, B. Temme, G. Erker, R. Frohlich and F. Zippel, *Organometallics*, 1997, **16**, 1440.
8 G. Talarico and P. H. M. Budzelaar, *Organometallics*, 2008, **27**, 4098.
9 W. C. McKee, J. Agarwal, H. F. Schaefer III and P. v. R. Schleyer, *Angew. Chem., Int. Ed.*, 2014, **53**, 7875.
10 J. Saßmannshausen, *Dalton Trans.*, 2014, **43**, 11195.
11 J. Saßmannshausen, J. Klett, A. R. Kennedy, J. A. Parkinson and D. Armstrong, *New J. Chem.*, 2013, **37**, 494.
12 J. Saßmannshausen, *Dalton Trans.*, 2011, **40**, 136.
13 R. Campbell, D. Cannon, P. García-Álvarez, A. R. Kennedy, R. E. Mulvey, S. D. Robertson, J. Saßmannshausen and T. Tuttle, *J. Am. Chem. Soc.*, 2011, **133**, 13706.
14 J. Saßmannshausen, *Dalton Trans.*, 2009, 8993.
15 S. Barnett, D. Allan, M. Gutmann, J. K. Cockcroft, V. H. Mai, A. E. Aliev and J. Saßmannshausen, *Inorg. Chim. Acta*, 2019, **488**, 292.
16 J. Saßmannshausen, *ACS Omega*, 2022, **7**, 35136.
17 J. E. Kickham, F. Guérin, J. C. Stewart and D. W. Stephan, *Angew. Chem., Int. Ed.*, 2000, **39**, 3263.
18 J. E. Kickham, F. Guérin, J. C. Stewart and D. W. Stephan, *Angew. Chem.*, 2000, **112**, 3406.
19 J. E. Kickham, F. Guérin, J. C. Stewart, E. Urbanska and D. W. Stephan, *Organometallics*, 2001, **20**, 1175.
20 N. Villegas-Escobar, J. Martínez, R. A. Matute, S. Saltarini, C. G. Daniliuc, L. H. Gade and R. S. Rojas, *Chem. Commun.*, 2021, **57**, 10327.
21 The used AIM2000 program assigns the sign to the original definition by Bader.
22 H. Shen, Z. Wang and M. Head-Gordon, *J. Chem. Theory Comput.*, 2022, **18**, 7428.
23 T. Ziegler and A. Rauk, *Theor. Chim. Acta*, 1977, **46**, 1.
24 T. Ziegler and A. Rauk, *Inorg. Chem.*, 1979, **18**, 1558.
25 M. P. Mitoraj, A. Michalak and T. Ziegler, *J. Chem. Theory Comput.*, 2009, **5**, 962.
26 IUPAC covalent bond: **https://goldbook.iupac.org/terms/view/C01384**.
27 IUPAC dative bond: **https://goldbook.iupac.org/terms/view/D01523**.
28 V. Vetere, C. Adamo and P. Maldivi, *Chem. Phys. Lett.*, 2000, **325**, 99.
29 J. P. Perdew, K. Burke and M. Ernzerhof, *Phys. Rev. Lett.*, 1996, **77**, 3865.
30 W. J. Hehre, R. Ditchfield and J. A. Pople, *J. Chem. Phys.*, 1972, **56**, 2257.
31 M. Dolg, U. Wedig, H. Stoll and H. Preuß, *J. Chem. Phys.*, 1987, **86**, 866.
32 M. Bühl and J. Saßmannshausen, *J. Chem. Soc., Dalton Trans.*, 2001, 79.
33 M. Bühl and H. Kabrede, *J. Chem. Theory Comput.*, 2006, **2**, 1282.

34 M. Bühl, C. Reimann, D. A. Pantazis, T. Bredow and F. Neese, *J. Chem. Theory Comput.*, 2008, **4**, 1449.
35 M. W. Schmidt, K. K. Baldridge, J. A. Boatz, S. T. Elbert, M. S. Gordon, J. H. Jensen, S. Koseki, N. Matsunaga, K. A. Nguyen, S. Su, T. L. Windus, M. Dupuis and J. A. Montgomery Jr., *J. Comput. Chem.*, 1993, **14**, 1347.
36 G. M. J. Barca, C. Bertoni, L. Carrington, D. Datta, N. De Silva, J. E. Deustua, D. G. Fedorov, J. R. Gour, A. O. Gunina, E. Guidez, T. Harville, S. Irle, J. Ivanic, K. Kowalski, S. S. Leang, H. Li, W. Li, J. J. Lutz, I. Magoulas, J. Mato, V. Mironov, H. Nakata, B. Q. Pham, P. Piecuch, D. Poole, S. R. Pruitt, A. P. Rendell, L. B. Roskop, K. Ruedenberg, T. Sattasathuchana, M. W. Schmidt, J. Shen, L. Slipchenko, M. Sosonkina, V. Sundriyal, A. Tiwari, J. L. Galvez Vallejo, B. Westheimer, M. Wloch, P. Xu, F. Zahariev and M. S. Gordon, *J. Chem. Phys.*, 2020, **152**, 154102.
37 N. Godbout, D. R. Salahub, J. Andzelm and E. Wimmer, *Can. J. Chem.*, 1992, **70**, 560.
38 R. F. W. Bader, *Atoms in Molecules: A Quantum Theory*, Clarendon Press, 1990.
39 E. D. Glendening, J. K. Badenhoop, A. E. Reed, J. E. Carpenter, J. A. Bohmann, C. M. Morales, P. Karafiloglou, C. R. Landis and F. Weinhold, *NBO 7.0*.
40 E. D. Glendening, C. R. Landis and F. Weinhold, *J. Comput. Chem.*, 2019, **40**, 2234.
41 F. Biegler-König, J. Schönbohm and D. Bayles, *J. Comput. Chem.*, 2001, **22**, 545.
42 F. Biegler-König and J. Schönbohm, *J. Comput. Chem.*, 2002, **23**, 1489.
43 *Jmol, Jmol: an open-source Java viewer for chemical structures in 3D*, **https://jmol.sourceforge.net/**.
44 T. Lu and F. Chen, *J. Comput. Chem.*, 2012, **33**, 580.